

Guessing the geometric features of a particle trajectory in a magnetic field by measuring one point and its tangent

Giuliano Parrini (Physics Dep. University and INFN Firenze, Italy)

Giuseppe Barbagli (INFN Firenze, Italy)

Fabrizio Palla (INFN Pisa, Italy)

Marco Meschini (INFN Firenze, Italy)

Acknowledgments: Didier Contardo (IPNL, Lyon)

Introduction: the geometrical issue

To determine the (~)helical trajectory of a charged particle in a uniform magnetic field (five parameters) the minimum information can be given by sampling one $R-\phi$ projected helix point plus one 3D point and the measurement of its tangent direction.

To do so two/three detector layers are needed depending on the tangent measurement method.

All that follows from pure geometrical considerations but how it is feasible in a real tracker detector?

This issue can be the base for the development of the silicon trackers from the nowadays useful recorder systems of sensors to intelligent, practical sensor systems.

Less parameters we need more easy is to give "local" and quick responses.

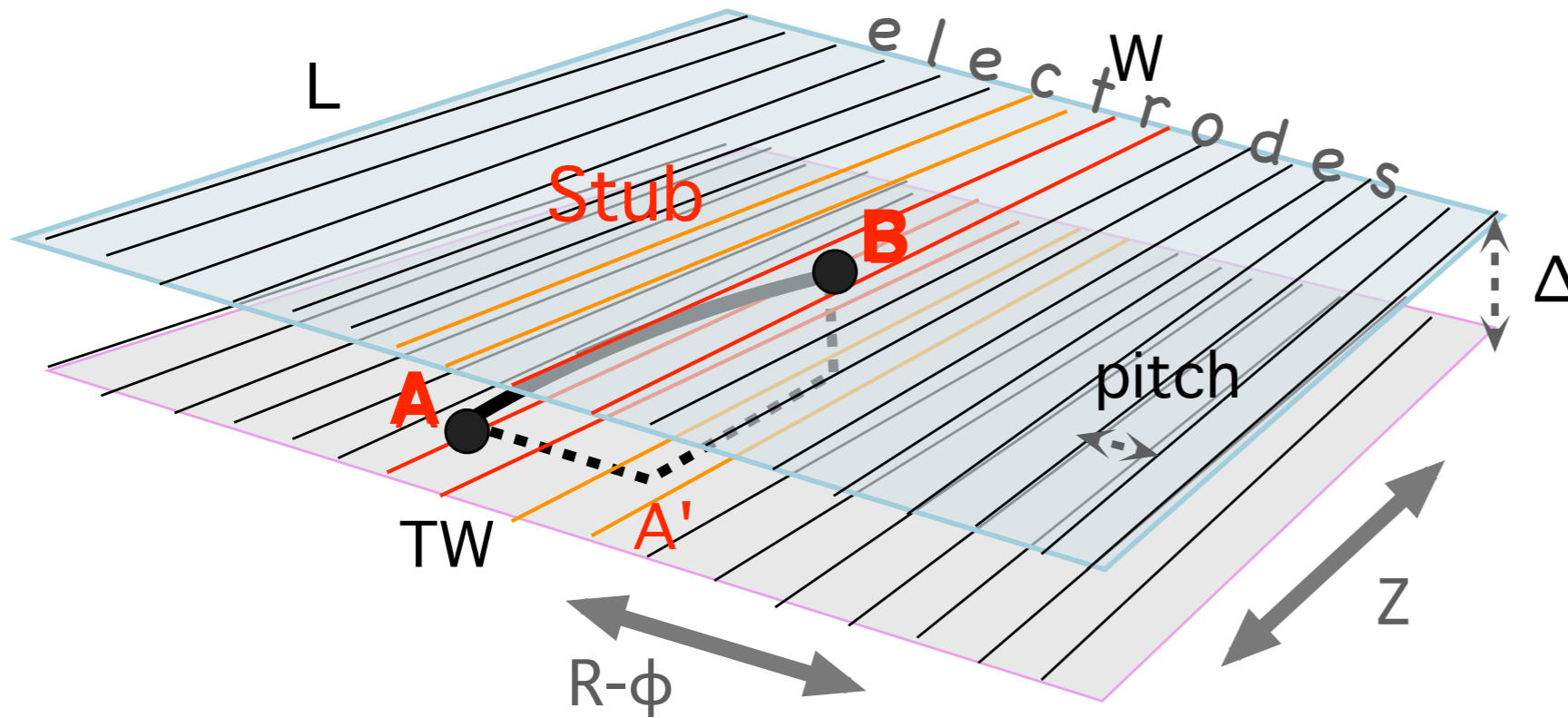
Introduction: the geometrical tangent

For the L1 trigger implementation it is of paramount importance that the radius (ρ) and the origin of the helix are known in very short time ($\sim 1 \mu\text{s}$).

The knowledge of the tangent direction (R- Φ projection) can be a good approach to the problem. In case the tracks come only from the interaction point (primary vertex) the discrimination of the tangent inclination allows the fast selection of high pTs. But in the real world the tangent inclination parameter selects also non primary particles of unpredictable pTs (e+e-, compton, secondary interactions,...) while still working correctly with primary tracks.

The measurement of one 3D point and its tangent gives a guess on the track pT because of the background haze, the certainty is reached only by correlations with few other detector layers. This assertion gives a first rough definition of the "local" concept.

The Stub Width measurement



$$TW = (n + x) \text{ pitch}$$

|
digitization
↓

$$TW_{\text{meas.}} = N \text{ pitch}$$

$$w = TW, p = \text{pitch}$$

$$TW_{\text{meas.}} = N \text{ pitch}$$

|
inversion
↓

$$N-2 < TW/\text{pitch} < N$$

$n = \text{Int}(w/p)$	fired strip probability (TW_{meas})			
	$N = 1$	$N = 2$	$N = 3$	$N = 4$
0	$1 - w/p$	w/p	0	0
1	0	$2 - w/p$	$w/p - 1$	0
2	0	0	$3 - w/p$	$w/p - 2$

TW : formulas and approximations (tracks from Z axis)

$$TW_r = TW / \Delta \approx f(pT^*, X/R)$$

“reduced” TW

$$pT_{\min} \text{ (GeV/c)} = 0.3 \text{ B(T) R(m)}/2 \quad ==\text{CMS}==> \quad 0.6 \text{ R(m)}$$

$$pT^* = pT/pT_{\min} \quad \text{“reduced” pT}$$

The scale factors allow a very synthetic description of Stub Widths

With $W/R < 0.2$ (angular acceptance) , $pT^* > \text{few units}$

$f(pT^*, X/R)$ is linear

flat layer
($pT^* = \infty$)

$$TW_r \approx \pm \left(\frac{pT_{\min}}{pT} \right) + x/R = \pm 1/pT^* + x/R$$

cylindrical layer

(pT^* any)

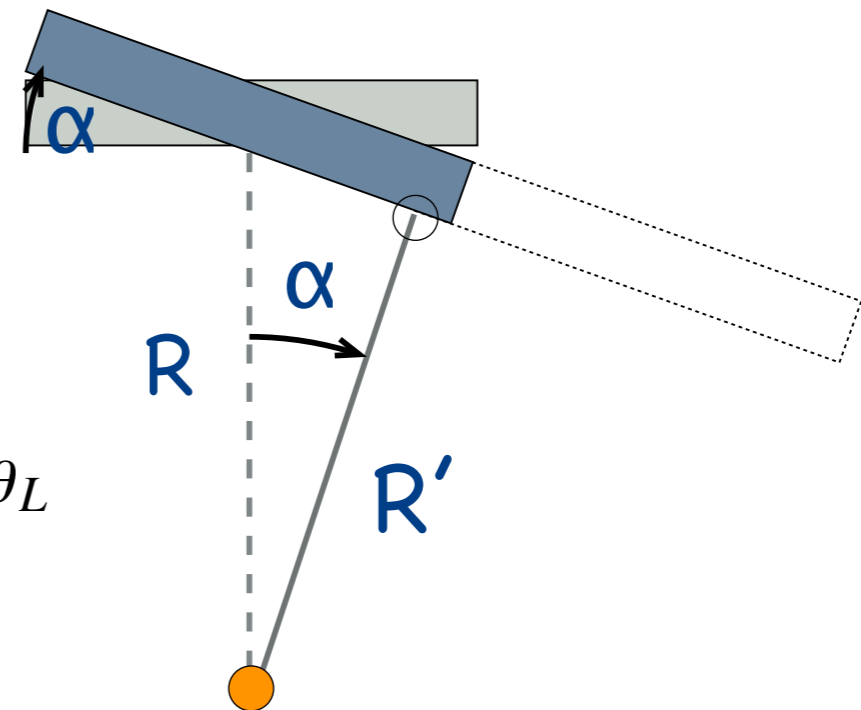
Lorentz spread compensation

The magnetic field effects on the signal charges inside the sensors produce a constant spread of TWs depending on the carriers (θ_L) and on the active thickness of the detector :

$$TW_r = \approx f(pT / pT_{\min}, X / R) + (2 D / \Delta) \tan \theta_L$$

2D is the effective path covered by the signal charges. In the single sensor case $2D = \Delta$, in the stacked case 2D is the full Si thickness or less. It depends on the relative position of the electrode meshes.

full compensation



general equation for the "linear" approx.

$$TW_r \approx \pm \left(\frac{0.6 R \cos \alpha}{pT} \right) + \tan \alpha + \frac{X}{R \cos \alpha} + (2 D / \Delta) \tan \theta_L$$

$$2 D = \Delta : \alpha = - \theta_L \quad 2 D < \Delta : \tan \alpha = - \frac{2 D}{\Delta} \tan \theta_L$$

TW measurements

reduced momentum $pT^* \geq 3$
 R- Φ acceptance $W/R < 0.2$
 full Lorentz compensation

$$\underbrace{\left(\frac{TW}{pitch} \right)}_{TW_{\text{measured}}} = TW_r \frac{\Delta}{pitch} \approx \left(\underbrace{\pm \left(\frac{1}{pT^*} \right)}_{\text{cylindrical layer}} + \underbrace{\frac{X}{R'}}_{\text{flat layer}} + \underbrace{\tan \alpha}_{\text{rotation}} + \underbrace{(2D/\Delta) \tan \theta_L}_{\text{Lorentz spread}} \right) \underbrace{\left(\frac{\Delta}{pitch} \right)}_{\text{ToP}}$$

ToP (Thickness over Pitch) is the new scale factor for the measurement amplitude

Real world : charge diffusion and capacitive coupling add a constant ($w_0 \leq 1$) which can depend on the amplitude discrimination of signals.

Lorentz angle (also Δ) varies with aging and it can be recovered tuning the bias voltage

pT selection : only 1/pT* term

Setting N strips as an upper limit (cut), the 100% efficiency of selection is achieved at

$$pT^* \Big|_{100\%} \approx \frac{1}{N-2} \times \frac{\Delta}{pitch}$$

while the full exclusion (0% efficiency) is either at or below

$$pT^* \Big|_{0\%} \approx \frac{1}{N-1} \times \frac{\Delta}{pitch}$$

In the range $\Delta pT^* = \frac{2}{(N-1)(N-2)} \times \frac{\Delta}{pitch}$ efficiency varies from 0% to 100%

- pT* threshold** increases with **ToP** and decreases with increasing N.
- N = 3** is the **minimum value** to reach **100% efficiency within a finite pT range**
- Real world:** $N \rightarrow \approx N-w0$

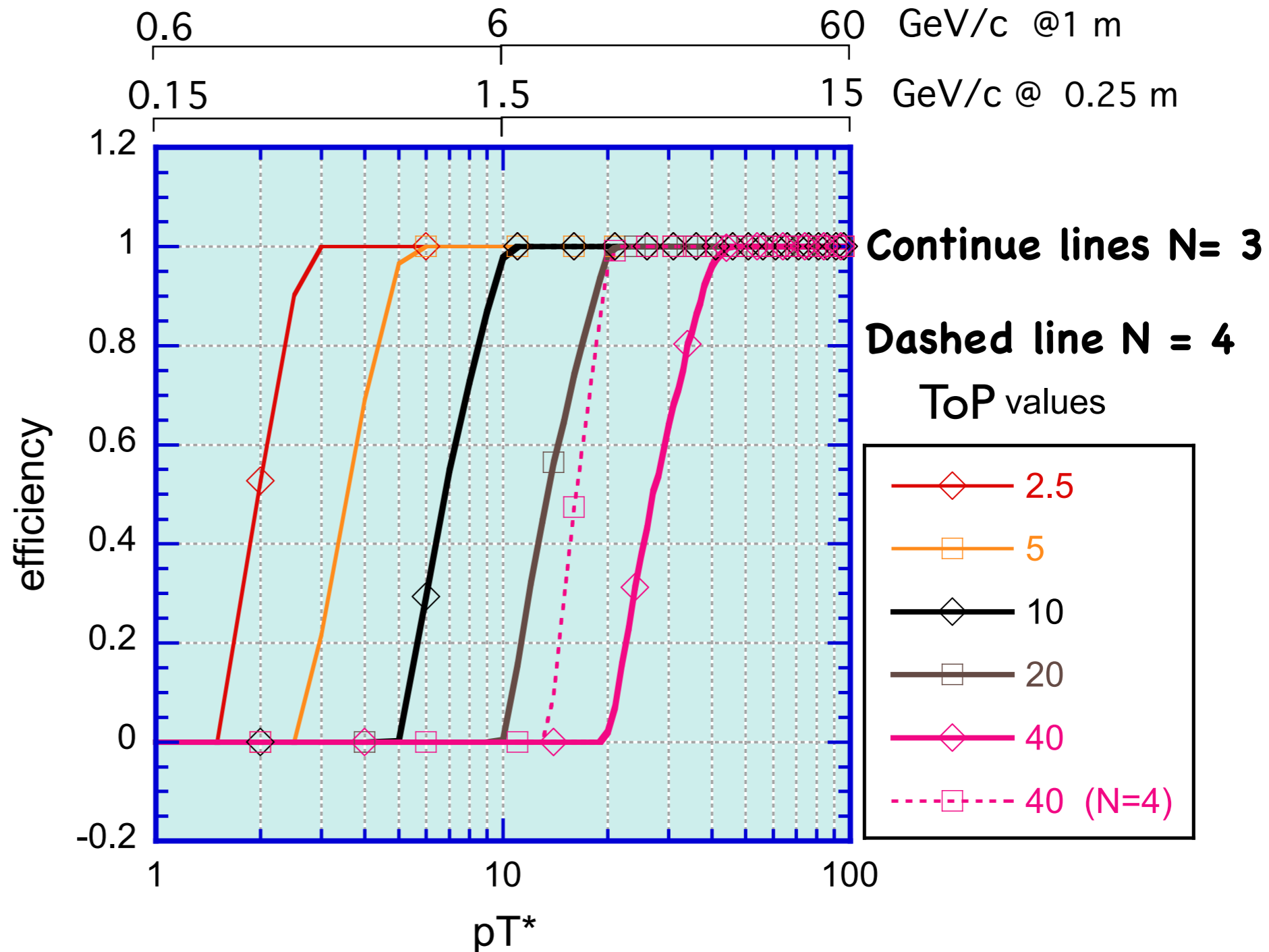
Selection efficiencies: $1/pT^*$ term

Numerically computed data confirm the formulas. Small discrepancies at $pT^* \approx \text{few units}$.

Computation has been made with very small angular acceptance ($X/R' \ll 1$)

For practical cases use
 $0.6 R(m) \times pT^*$
 (4 T magnetic field)

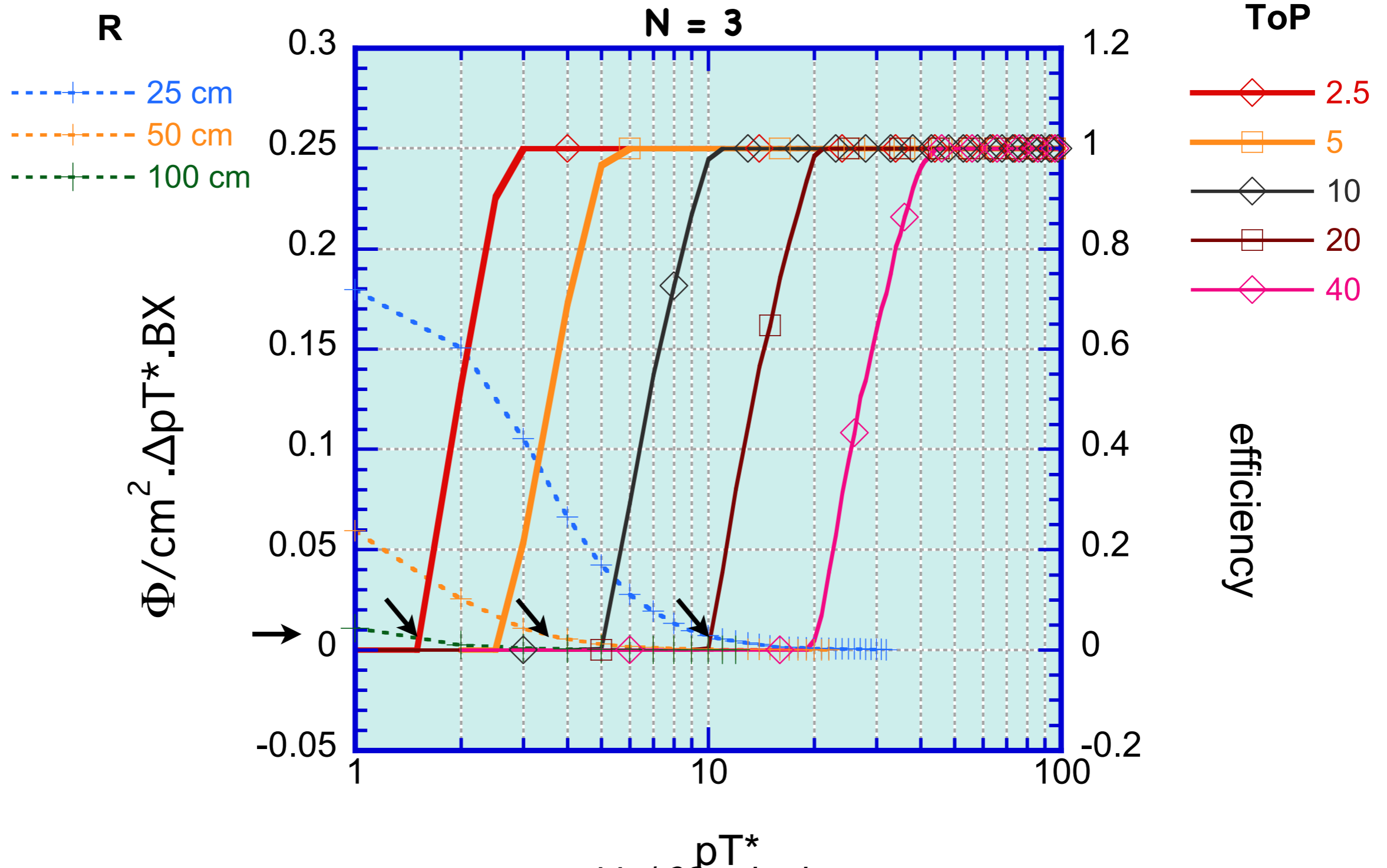
At $pT^* > \text{few units}$
 (linear approx.)
 curves are described by
 $\text{eff} \approx (N-1) - \text{ToP}/pT^*$





The barrel layout: primary Background

To estimate the p_T threshold to reduce the minimum bias rate I compare the selection curves with the flux obtained (4×10^4 particles/ 4π /BX) in a 4 T magnetic field at $\eta \approx 0$.





The detector layout: secondary background

Big issue, not to exhaust in a couple of slides!

Electrons, nuclear interactions,.. have an unpredictable origin.

The Stub widths they produce are

$$TW_r \approx \pm \left(\frac{0.6 R_b}{pT'} \right) + \frac{X - X_0}{R_b} \quad (\text{Lorentz spread compensated?})$$

R_b , X_0 are the origin coordinates wrt the detector of the particle with pT' momentum.

If particles are generated at R' from the detector their pT' upper limit is

$$pT' \leq \frac{N-2}{N-1} \times \frac{R_b}{R_0} \times pT_{100\%} \quad \left(pT' \leq \frac{1}{2} \times \frac{R_b}{R_0} \times pT_{100\%} \right) \leftarrow \text{N} = 3$$

The pT' limit decreases with the approaching of the origin to the detector ($R' \rightarrow 0$) and increases with the increasing of the threshold of the primary particles.

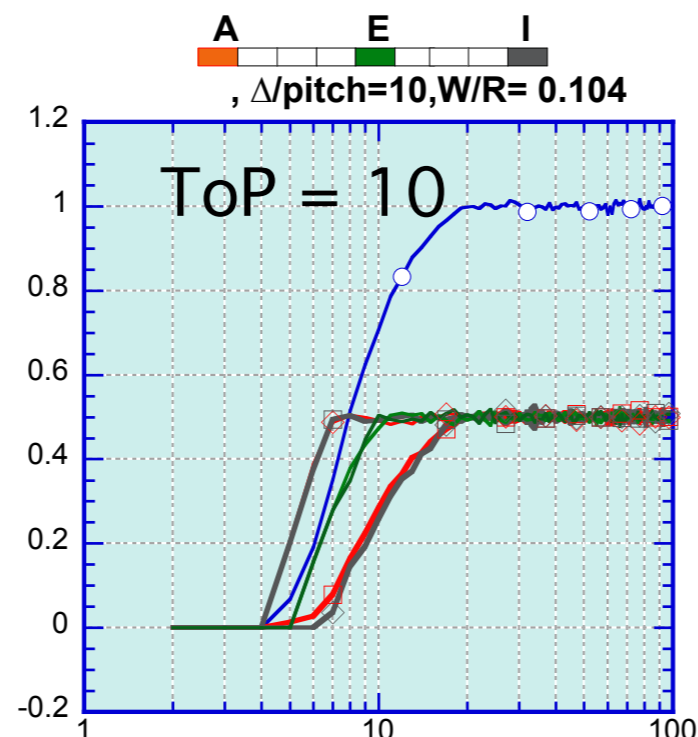
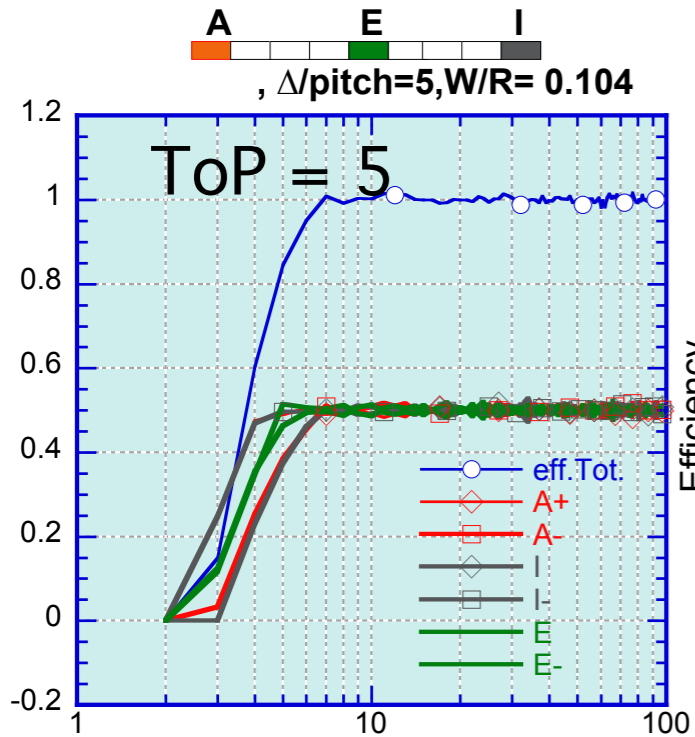
Can these simple remarks imply some constraints for the layout?

e.g.the spacings between successive layers which should not be equals.

Selection efficiency: including the X/R' term

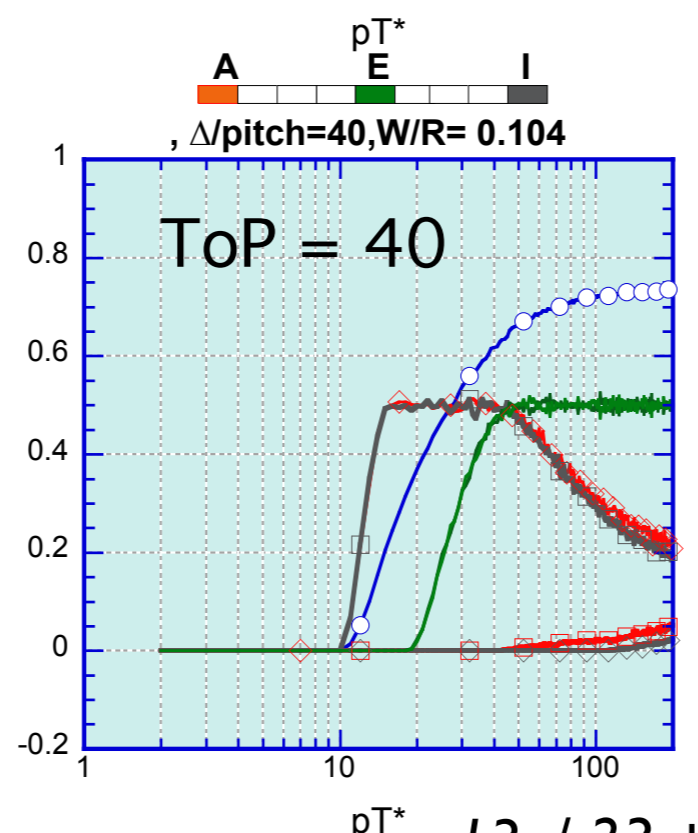
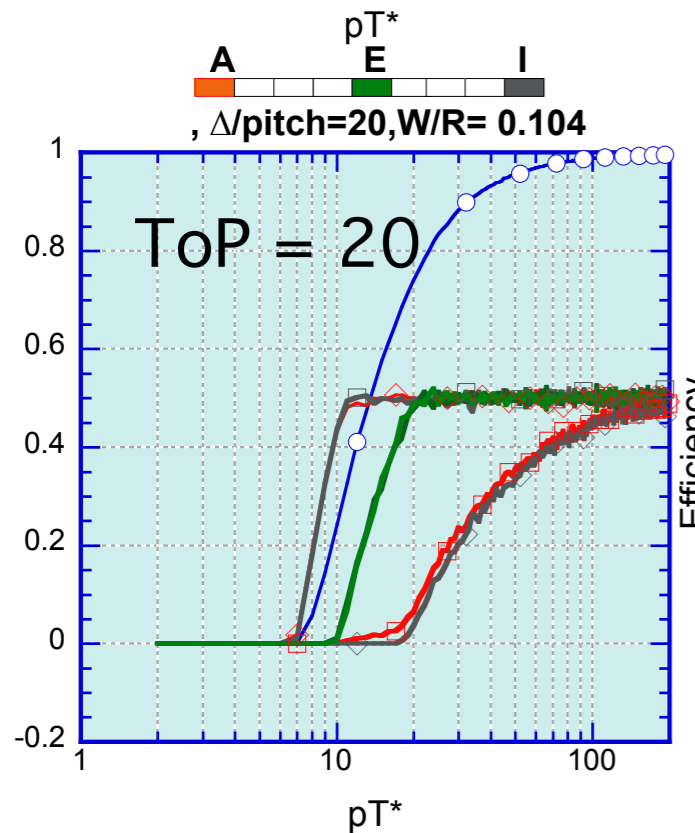
When $X/R' \approx 1/pT^*$ the simple width discrimination fails

(angular acceptance $\cong 1/pT^*$ threshold, High thresholds and large acceptances)



$N = 3$, Lorentz compensated

detectors are divided into 10 regions A,B,...,I
 single region efficiencies are divided by charge sign and normalized to the total number of particles



- total efficiency ($W/R \approx 0.1$)
- central efficiency ($W/R \leq 0.01$)
- left side efficiency
- right side efficiency

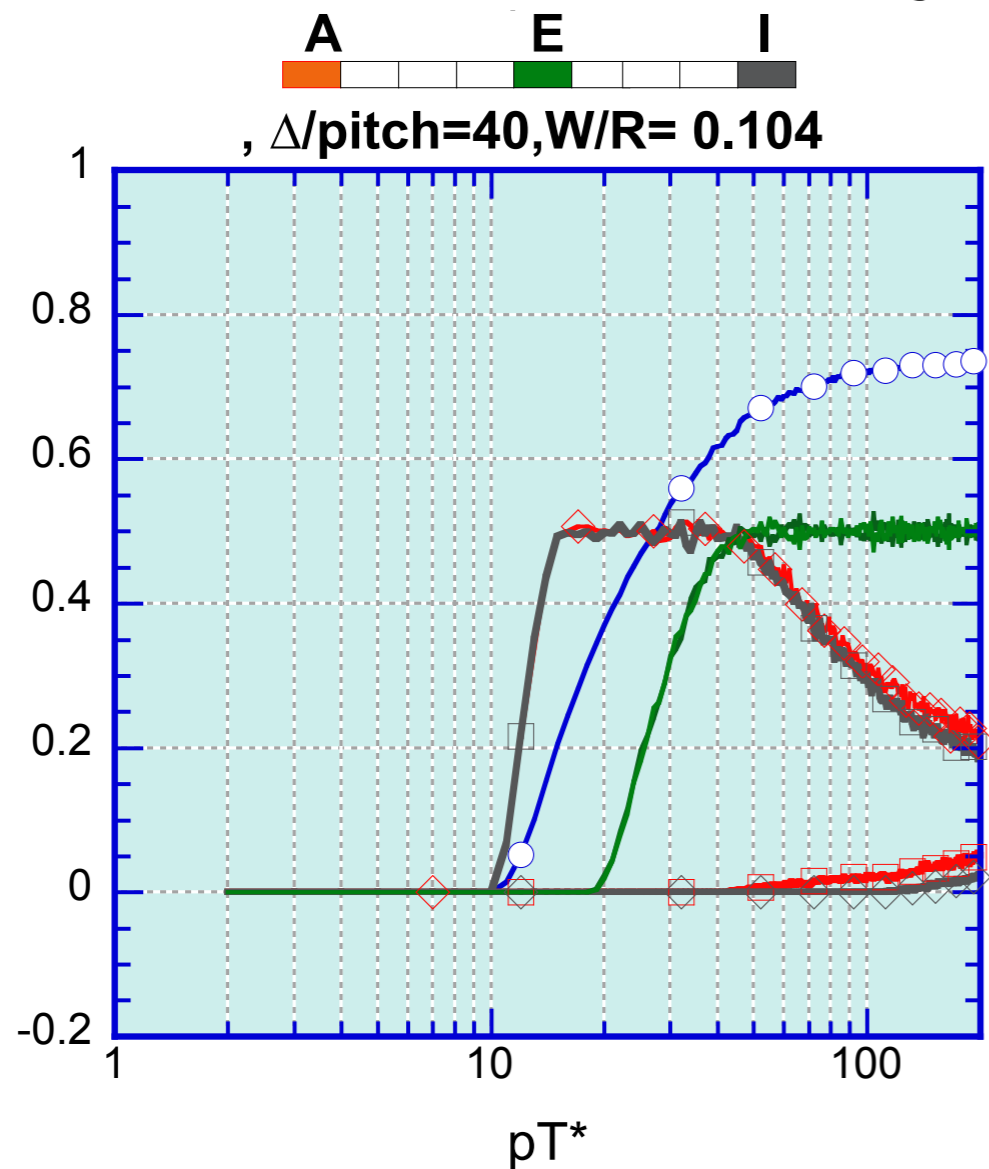
The X/R mapping (on detector)

Two possibilities for the rounding of the X/R correction: up to the next integer (Excess approximation), down to the nearest integer (Defect approximation).

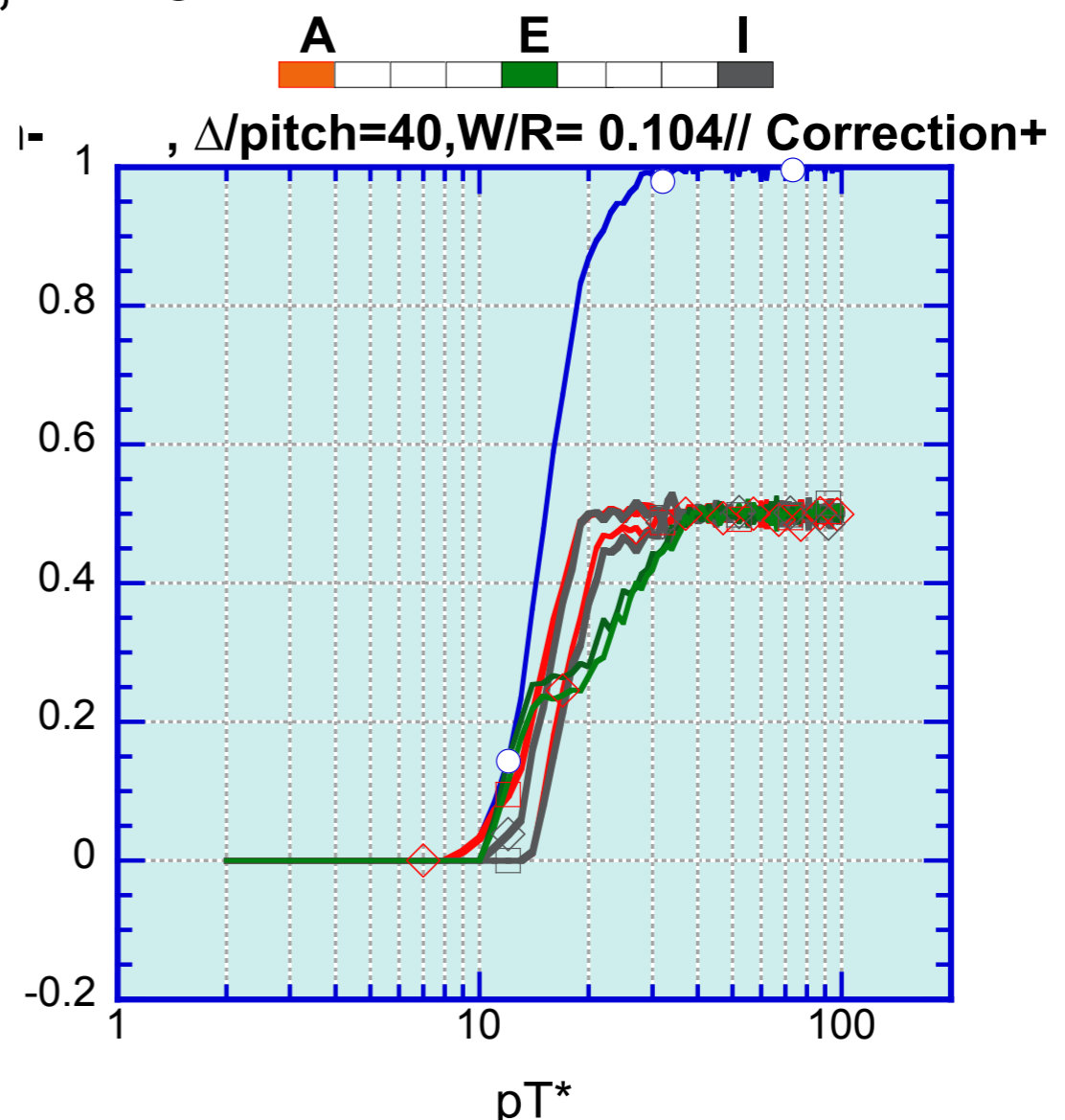
A few concerns about the homogeneity of the selection remain.

100% threshold is higher.

ToP = 40, N = 3



no corrections



correction map (excess approx.)

The endcap region : slabs normal to Z

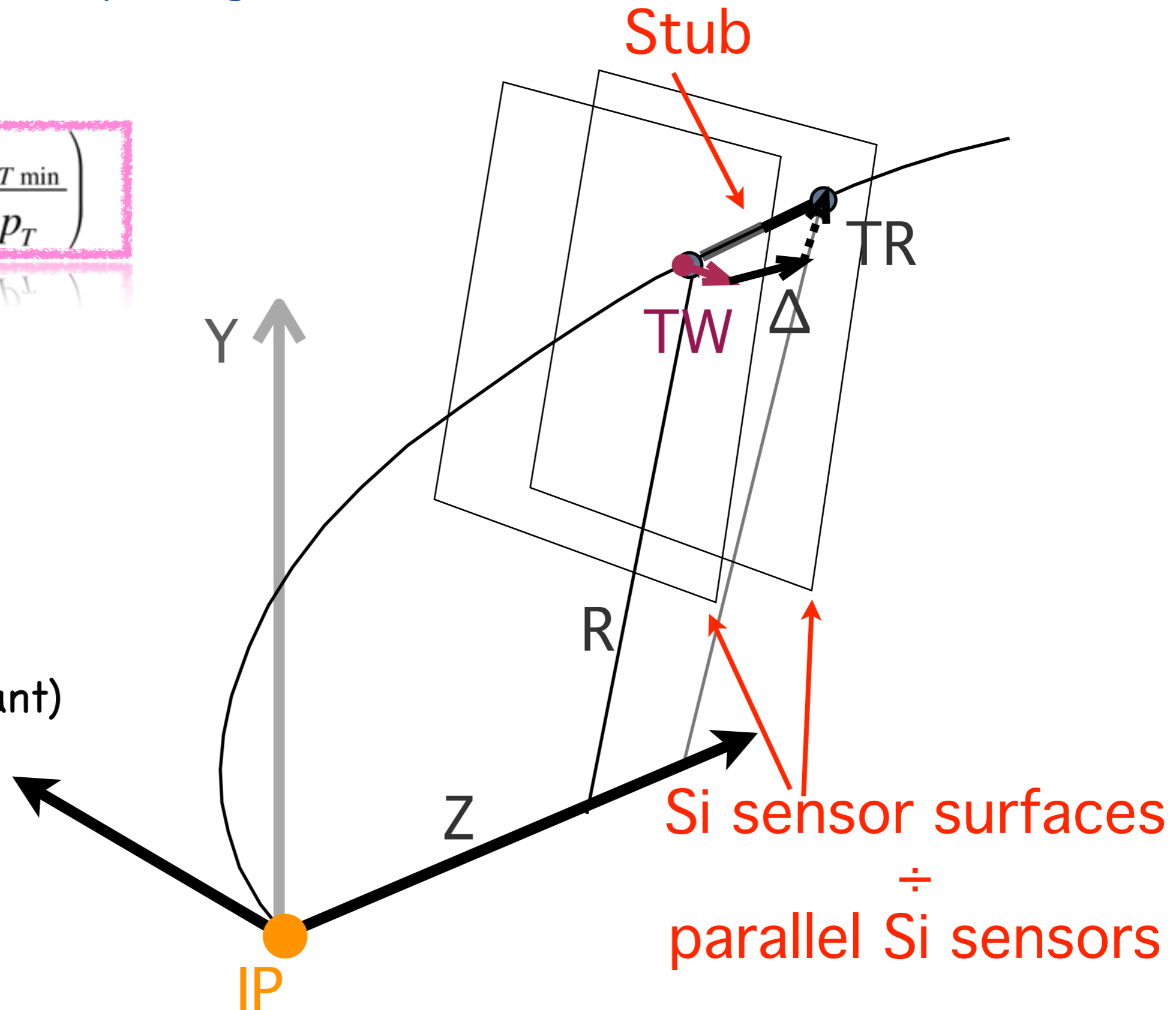
$$\frac{TW}{R} = -\frac{\Delta}{Z} \sin^{-1}\left(\frac{p_{T \min}}{p_T}\right)$$

$$p_{T \min} = 0.6 R$$

(B = 4 T, R(m))

No "tile" effects
(but R is not constant)

No Lorentz drift



Stub width measurements

$$\frac{TW}{pitch} \approx - \frac{\Delta}{pitch} \frac{R}{Z} \frac{p_{T\min}}{p_T}$$

For $p_T \geq 0.5 p_{T\min}$

Similar to the barrel case with small acceptance sensors and no Lorentz drift.

$R (p_{T\min})$ varies from point to point on all the disk plane .

Some attention is required for the sensor segmentation (strips, ministrip,..). The proper strip symmetry is radial, but with $< 10 \times 10 \text{ cm}^2$ detectors a parallel symmetry should introduce acceptable distortions at $R \geq 50 \text{ cm}$ or less. In the following I assume a constant ratio $\Delta/pitch$ (ToP) as in barrel case

$$\frac{TW}{pitch} \approx - \frac{\Delta}{pitch} f \frac{1}{p_T^*} , \quad f = \frac{R}{Z}$$

pT selection threshold

As in the barrel case, the stub widths $< N$ give pT selections of the type:

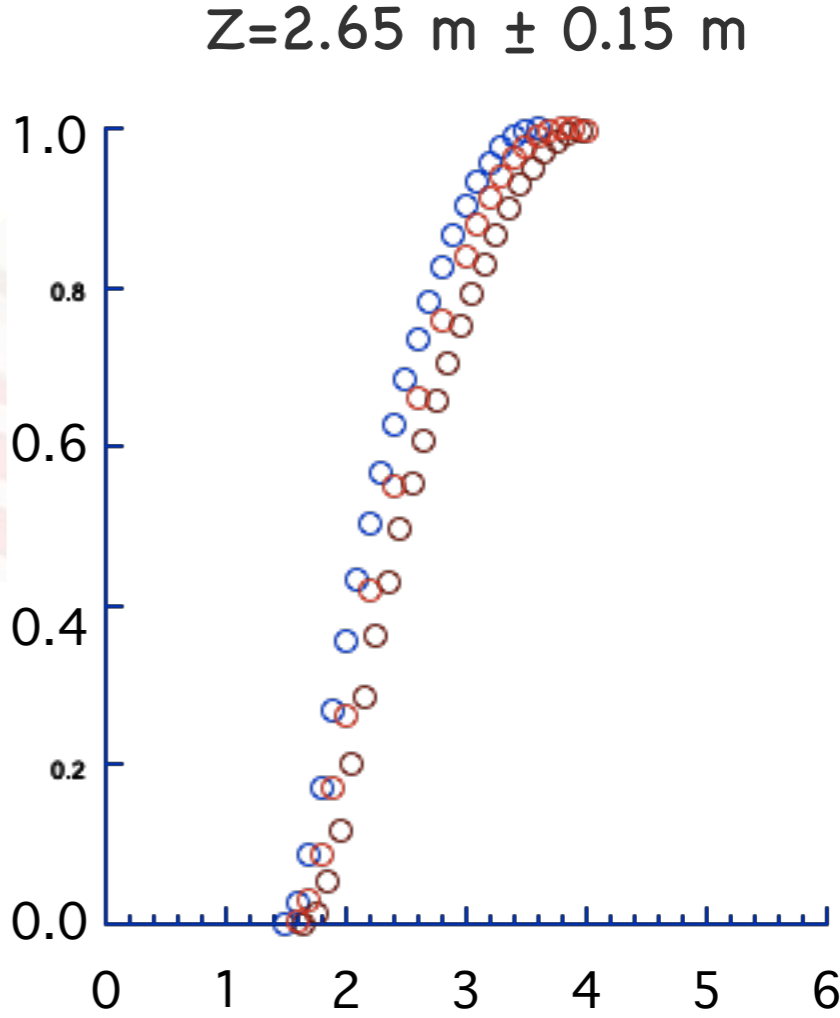
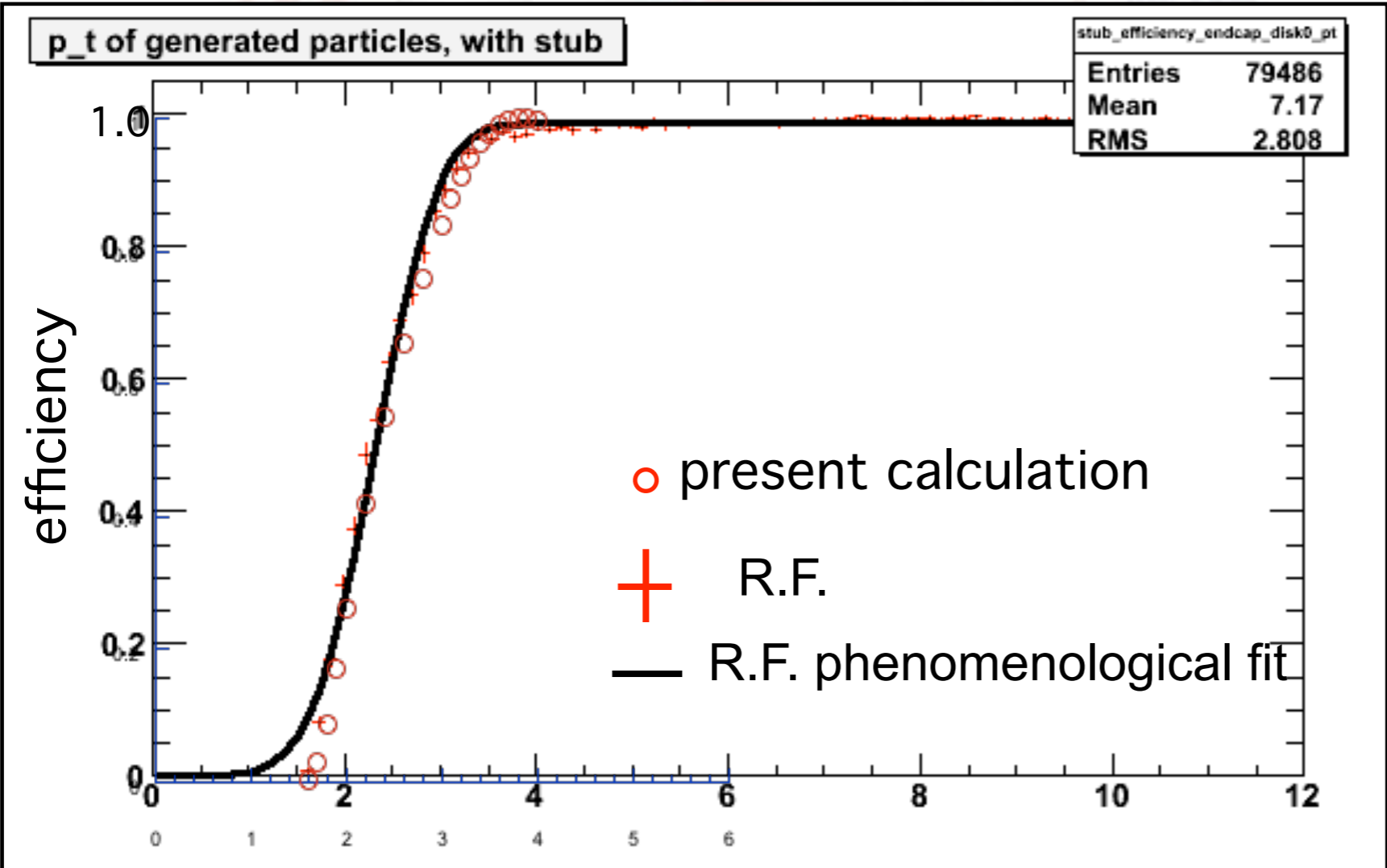
$$pT^*|_{100\%} \Rightarrow pT|_{100\%} \approx \frac{1}{N-2} \times \frac{\Delta}{pitch} \times f \times pT_{\min}$$
$$pT^*|_{0\%} \Rightarrow pT|_{0\%} \approx \frac{1}{N-1} \times \frac{\Delta}{pitch} \times f \times pT_{\min}$$

$f = R/Z$ is usually < 1 and hence higher ToPs are needed to perform pT cuts similar to those of the barrel.

To keep about the same pT threshold ToP must be changed from disk to disk and from ring to ring.

pT thresholds vary inside the detector from R_{IN} to R_{EXT} and we expect that efficiency curves are less steep than those in barrel detectors.

Disk at $Z= 2.65 \text{ m}$, $83 \text{ cm} \leq R \leq 96 \text{ cm}$, $ToP = 20$, $N=3$



Robert Frazier 21/01/10, numerical computation

pT (GeV/c)

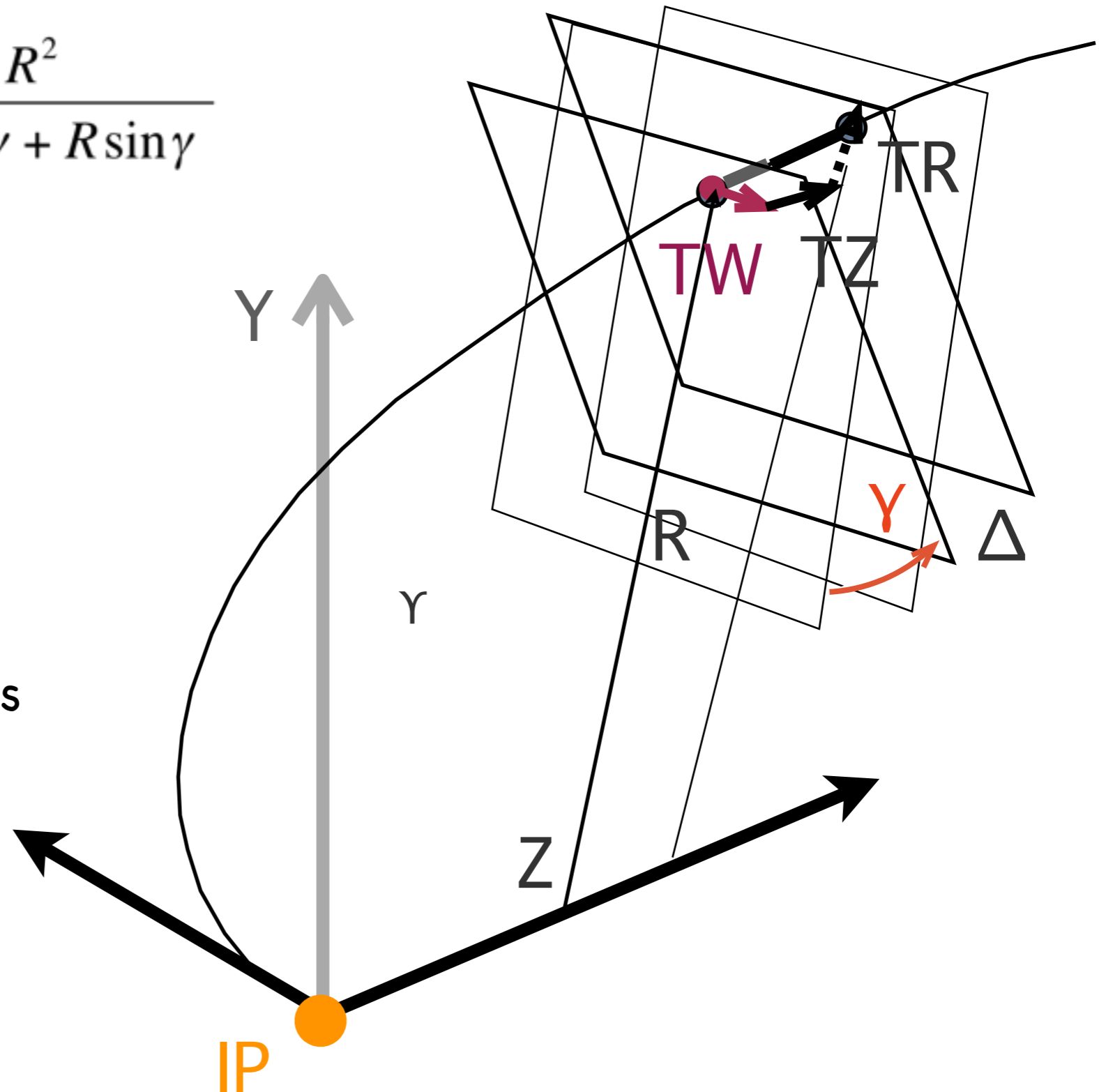
The general case of inclined slabs

$$TW \approx -\Delta \frac{0.6}{p_T} \frac{R^2}{Z \cos \gamma + R \sin \gamma}$$

$$TW \approx -\Delta \frac{0.6}{p_T} R_{eq}$$

$$R_{eq} = \frac{R^2}{Z \cos \gamma + R \sin \gamma}$$

“tile” and Lorentz drift effects
not taken into account...
...but smaller than in the
barrel case

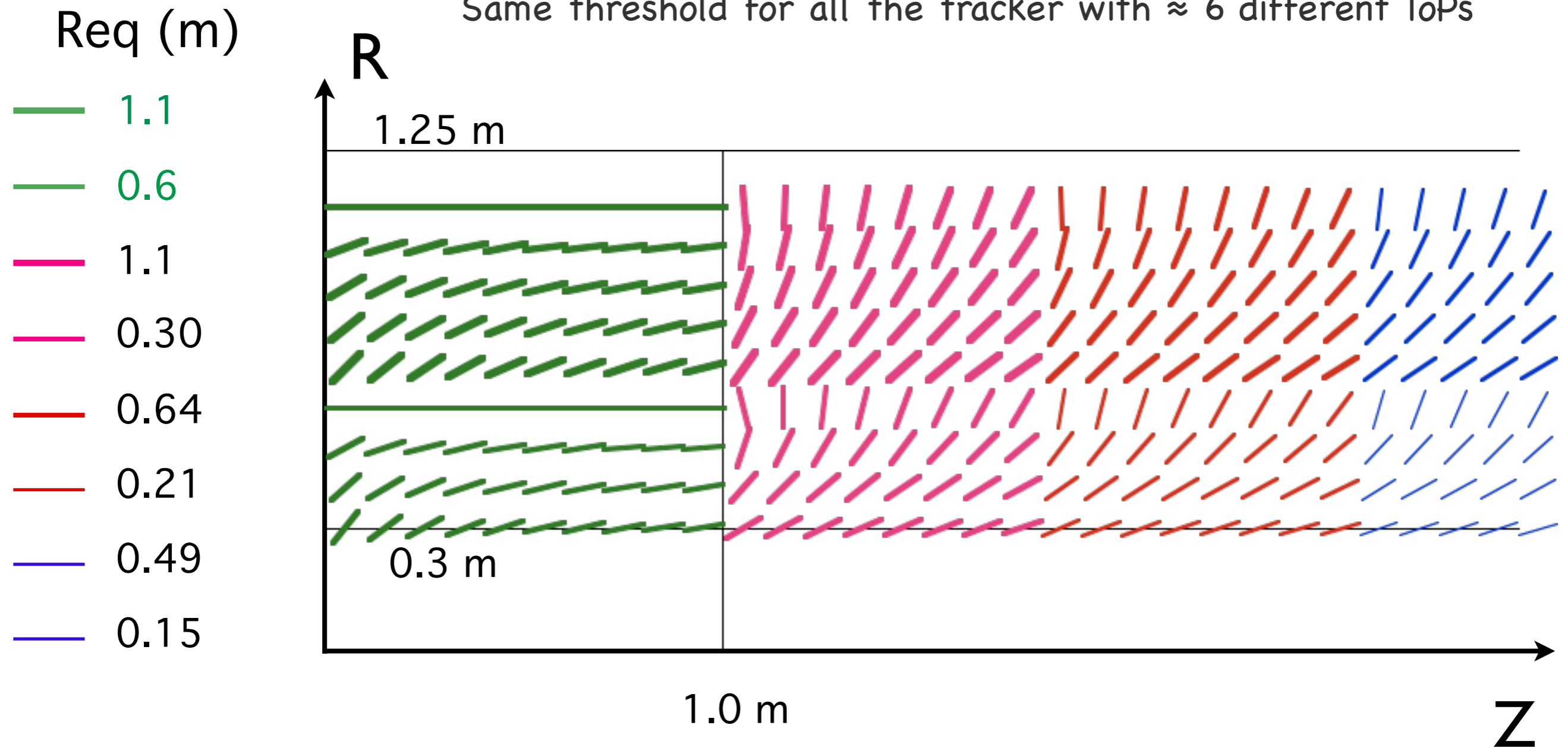


R-Z map (10x10 cm²) : disc/barrel like geometry (not a layout proposal)

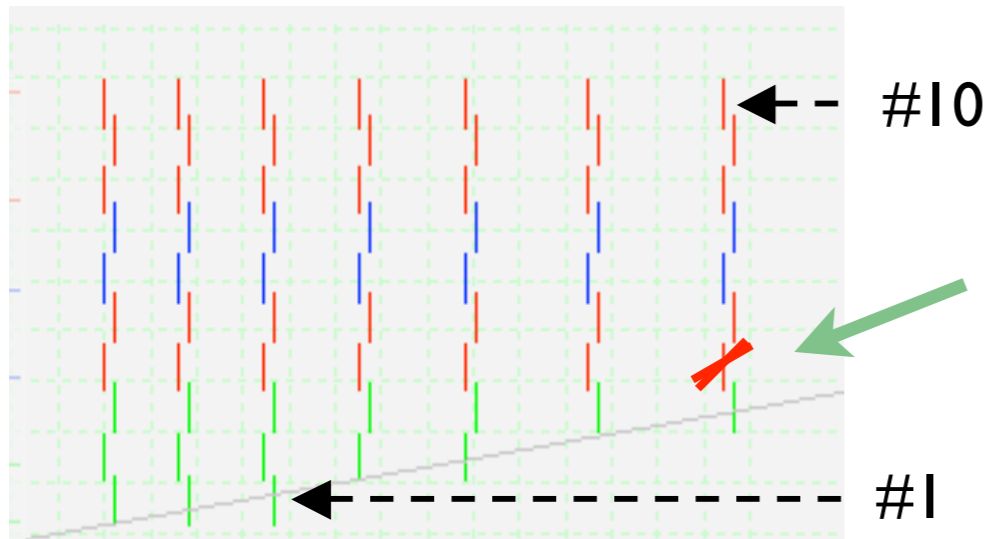
$$pT_{th100\%} = ToP \times 0.6 \text{ Req} \quad , \quad TW \leq 2 \text{ strip (N = 3)}$$

Within each region (8), same detectors and same pT threshold.

Same threshold for all the tracker with ≈ 6 different ToPs

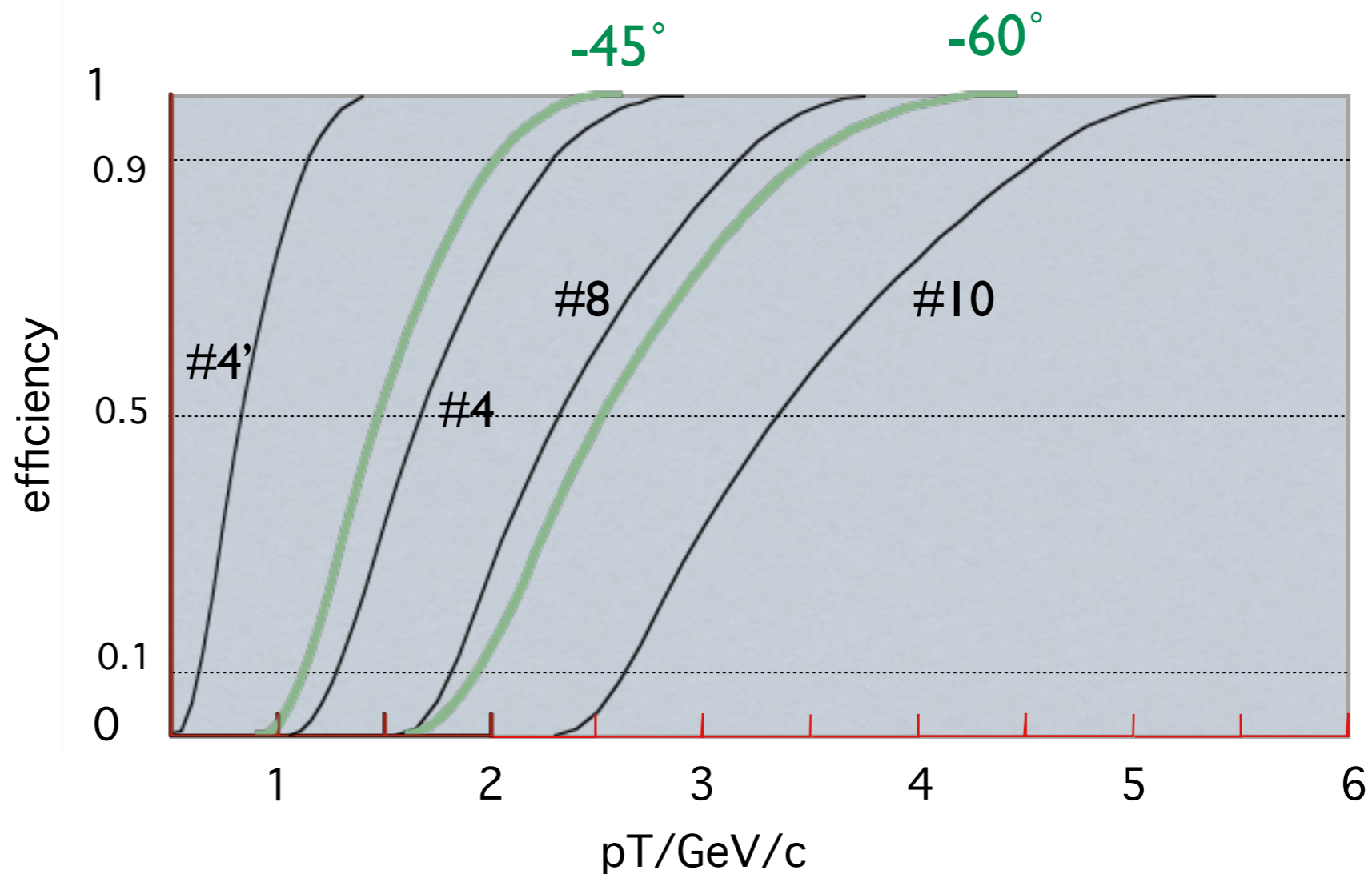


Disk 7 , rings #10, 8, 4 (ref. R.Frazier) cut at $N = 3$



modules of the 4th ring with the ToP of the 8th, 10th rings are tilted in R-Z

#4 has twice the ToP of #8 , #10
#4' the same ToP



Discussion I

The measurement of p_T s of tracks crossing a single detector of the tracker can be done directly by measuring the “stub” $R-\Phi$ widths produced. This is true for tracks coming from primary vertex. To avoid spurious triggers correlations one can use additional information coming from nearby detectors. The main characteristic of the stub width is the proportionality to $1/p_T$ and its scalability with the detector position and geometry.

Tile geometry of the sensors and Lorentz drift can affect the selection introducing perturbations of the $1/p_T$ behavior which depends on the geometry of the layout.

Inside the same detector layout the scale factors depend on the position of the detector and on its structural “thickness-over-pitch” (ToP) specs. Several R&D activities are investigating the convenient ToP values to be used for the p_T selection as well as the best way of obtaining them.

The non primary background suggests to correlate p_T selections on different tracker layers. That could require the use of similar p_T thresholds and hence different ToPs since thresholds depend on the radial position as well as on Z position (endcaps).

Discussion II

The layouts usually considered are the barrel geometry, mostly in the central region, and the disc geometry at the end caps of the tracker. In this presentation I pointed out that in a variable layout scheme the radial and Z dependence of the p_T threshold can be compensated by a suitable inclination of the detector with respect the Z axis. This method should allow to have same p_T threshold in wider regions of the tracker simply exploiting sensors with the same ToP .

The cons of this approach must be evaluated. Effects due to the finite sensor tiles, to the primary interaction vertex spread, etc. must be investigated. Mechanics issues may play an important role too.

If all these cons were "easily" surmountable, selections based on correlations among different (R- Φ) sensors would be facilitated.

Backup

abstract

The talk reviews the geometric basis of the "PT" and "CW" approaches for the selection of high transverse momentum particles coming from primary interactions at sLHC. Starting from the definition of a small segment measurement (stub) of a particle trajectory it gives basic general constraints which contour the architecture of both methods. The sensor position with respect to the production vertex as well as the sensor structure and design are key factors the behavior of which is described by a-dimensional parameters according simple scaling laws. Using these tools the selection efficiency of high transverse momentum is discussed in a thorough way, with emphasis to the effects due to the Lorentz drift, non primary background particles, sensor dimension and position. The discussed predictions, while waiting the LHC collisions validation, can be verified with the cosmic rays data in the CMS Tracker.

Measurements of the Helix parameters

3 D sample (∞^1 solutions)

(X_1, Y_1, Z_1) :
two equations

geom. tangent (X_1, Y_1, Z_1) :
two equations

$$(X_1 - X_0) = \rho \cos\left(2\pi \frac{Z_1 - Z_0}{p}\right)$$

$$(Y_1 - Y_0) = \rho \sin\left(2\pi \frac{Z_1 - Z_0}{p}\right)$$

$$\frac{dx}{dz} = -2\pi \frac{\rho}{p} \sin\left(2\pi \frac{Z_1 - Z_0}{p}\right)$$

$$\frac{dy}{dz} = 2\pi \frac{\rho}{p} \cos\left(2\pi \frac{Z_1 - Z_0}{p}\right)$$

2 D sample (R- ϕ projections) (∞^3 solutions)

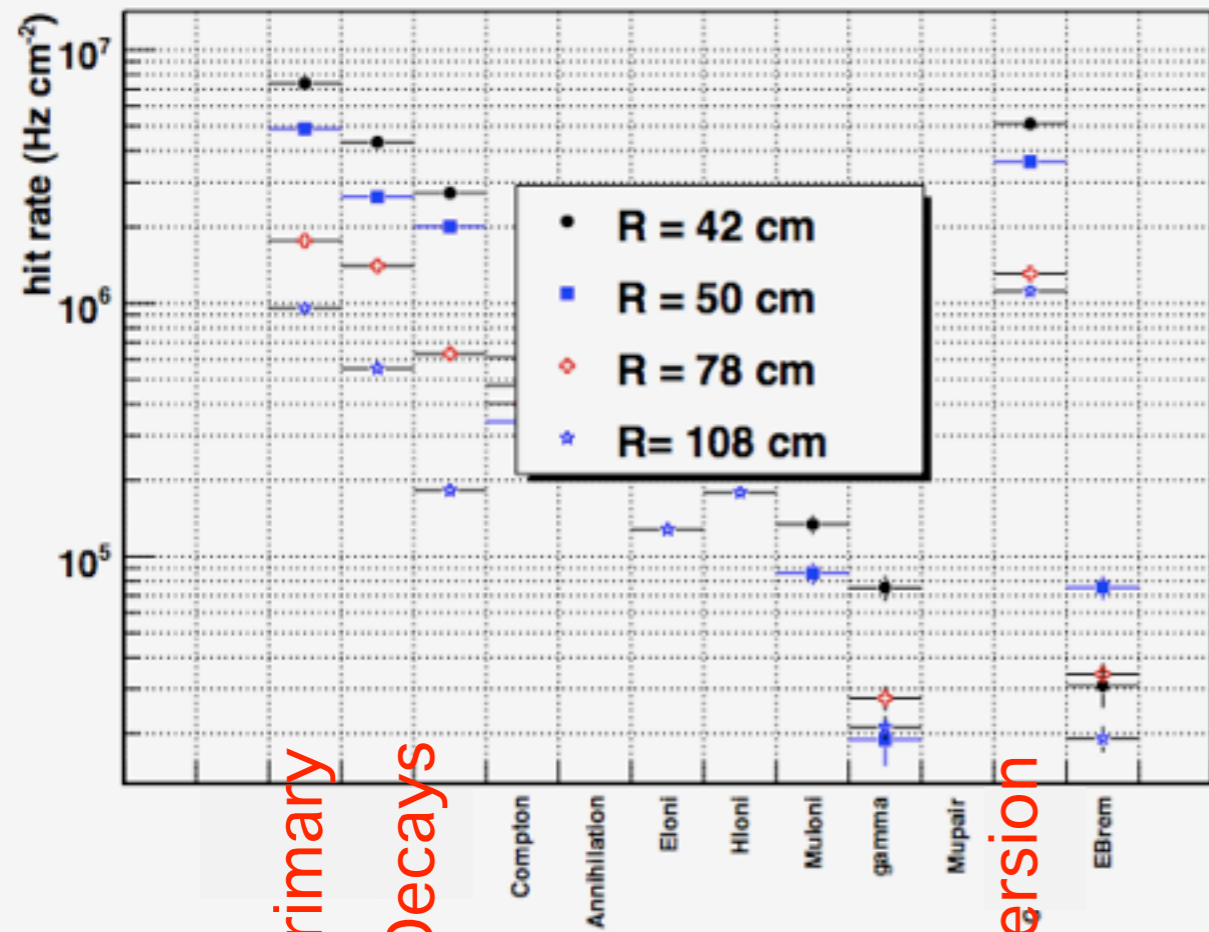
(X_1, Y_1) :
one equation

geom. tangent (X_1, Y_1) :
one equation

$$(X_1 - X_0)^2 + (Y_1 - Y_0)^2 = \rho^2$$

$$\frac{dy}{dx} = -\left(\frac{X_1 - X_0}{\rho}\right) \frac{1}{\sqrt{1 - \left(\frac{X_1 - X_0}{\rho}\right)^2}}$$

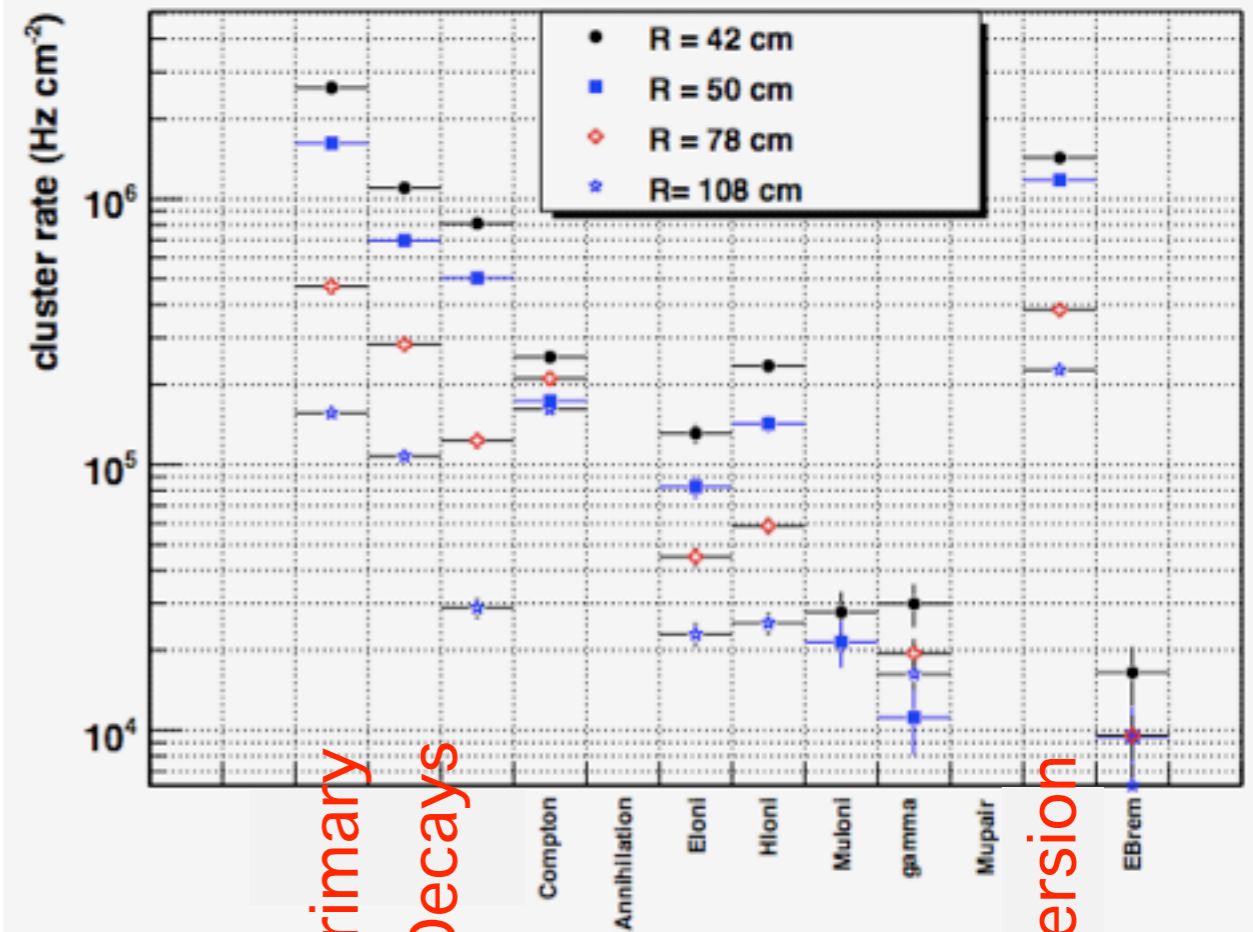
Data rate in Barrel - I (F.Palla)



Primary

Hadronics+Decays

Conversion



Primary

Hadronics+Decays

Conversion

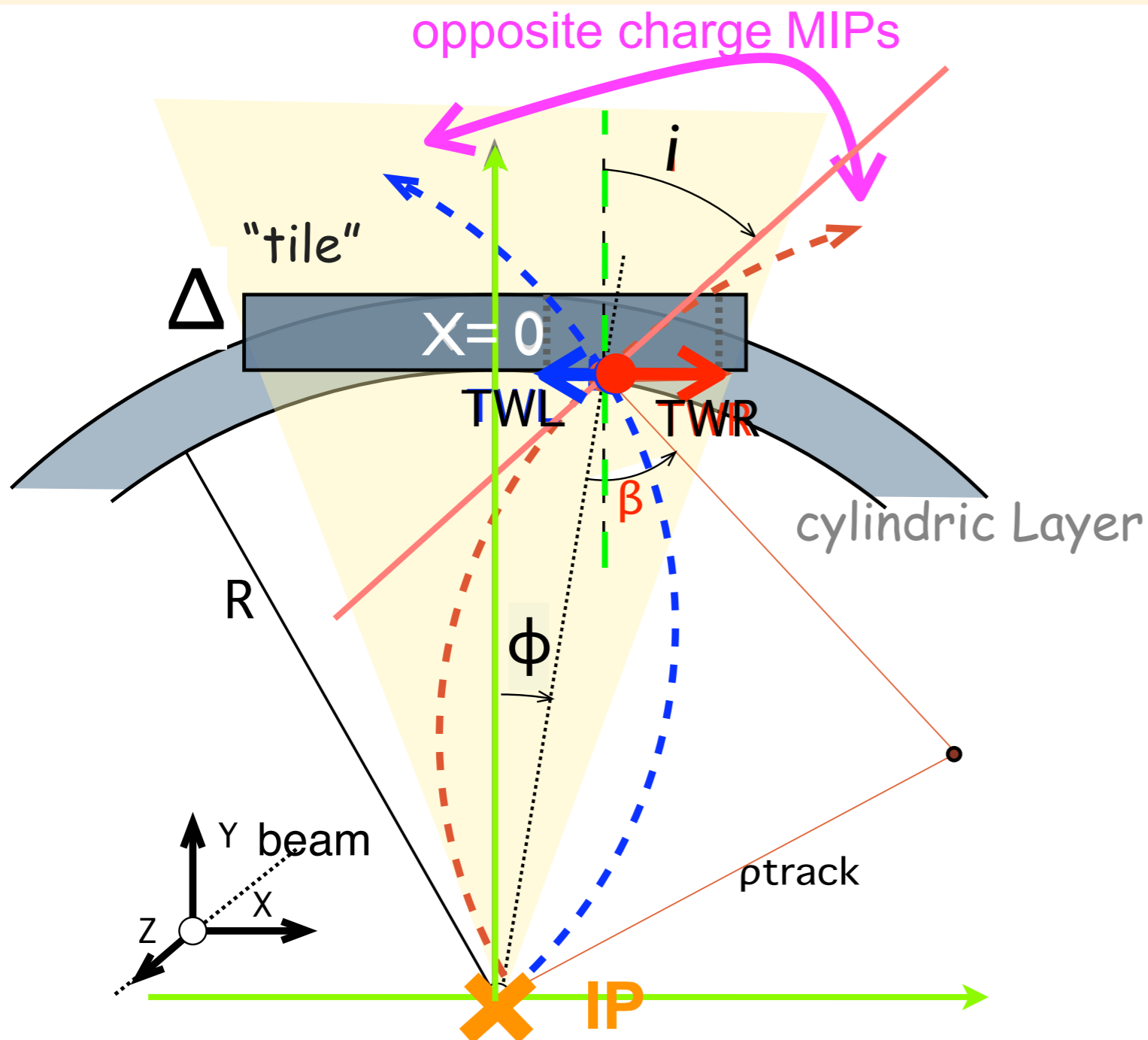


The "stub" width (TW)

Dependence on detector parameters and on the curvature of the helix quite complicate.

$$\text{If } TW^2 + \Delta^2 \ll \rho_{\text{track}}^2$$

$$TW/\Delta \approx \tan i$$



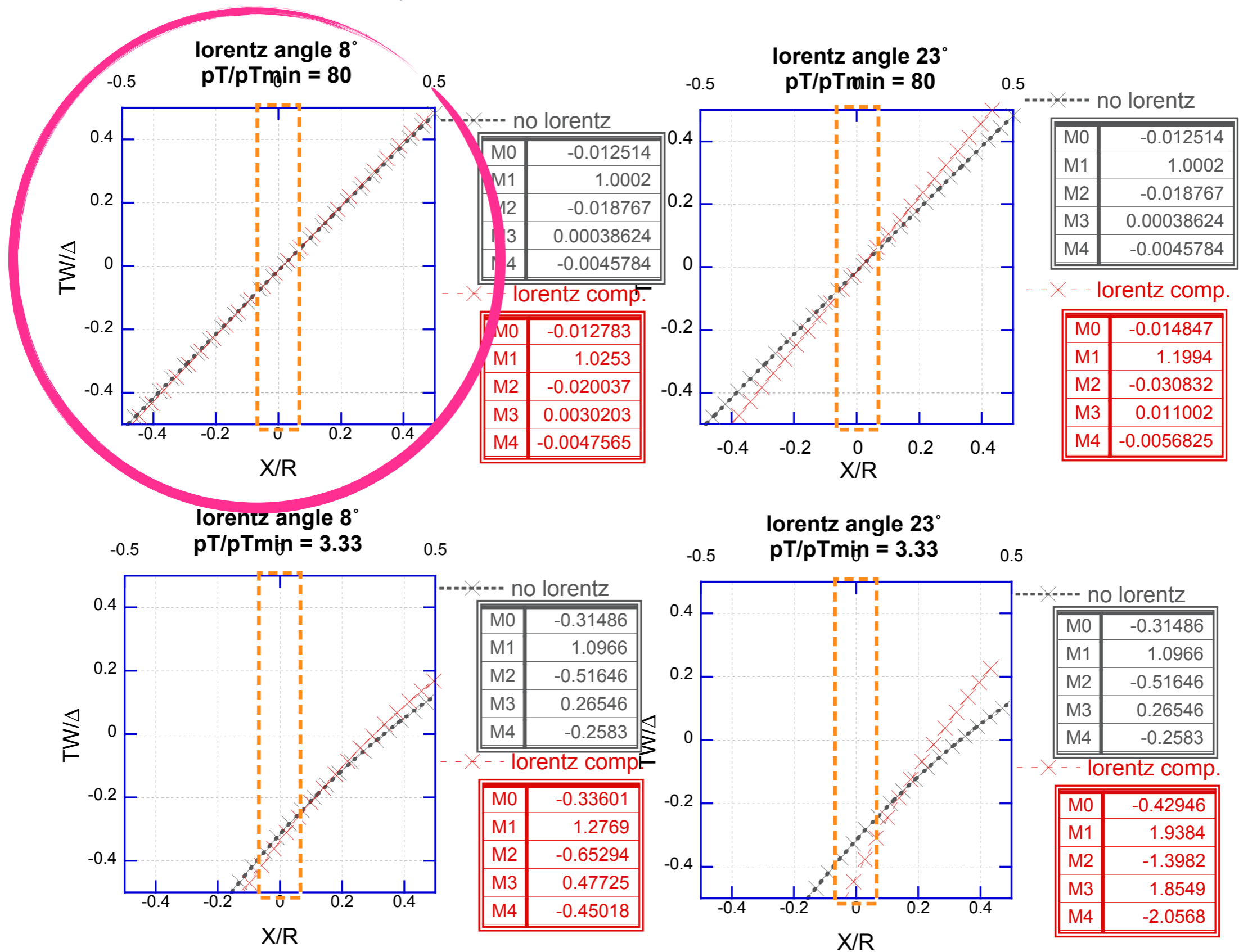
$$\tan i = \cot \beta \frac{1 + \tan \beta \tan \phi}{1 - \cot \beta \tan \phi}$$

$$\cot \beta = \sqrt{\frac{1 + (x/R)^2}{(pT/pT_{\min})^2 - 1 - (x/R)^2}}$$

$$pT_{\min} = 0.6 R \quad (B = 4 \text{ T, } R/\text{m})$$

$$\tan \phi = x/R$$

compensation by rotation

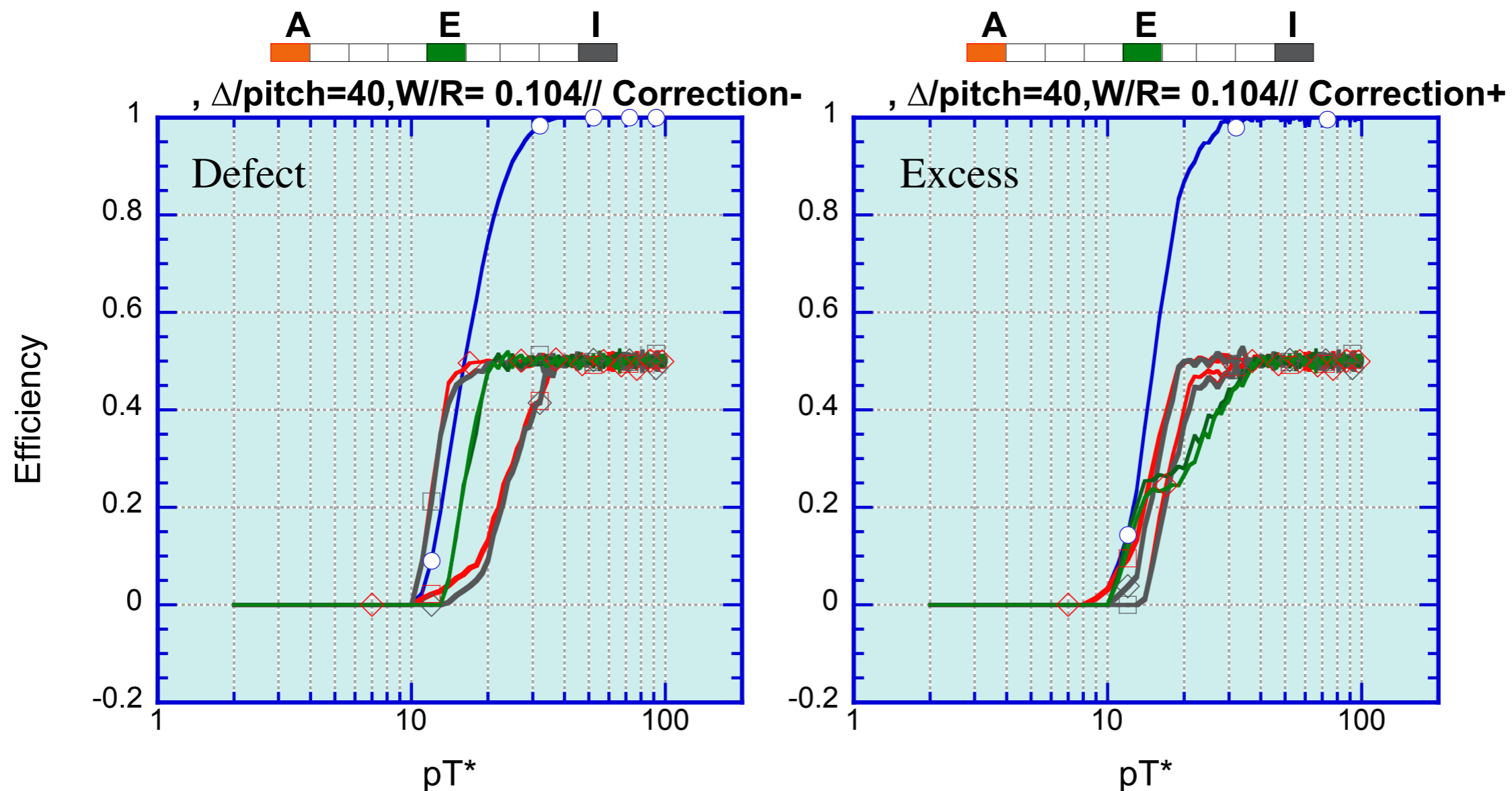


High thresholds : the map of the detector

Large acceptances require to map the detector by subtracting the X/R term. This is possible in the stacked detectors where the sign of stubs is known.

Two possibilities for the rounding of the X/R correction: up to the next integer (Excess approximation), down to the nearest integer (Defect approximation).

Few concerns about the homogeneity of the selection remain. 100% threshold is higher.

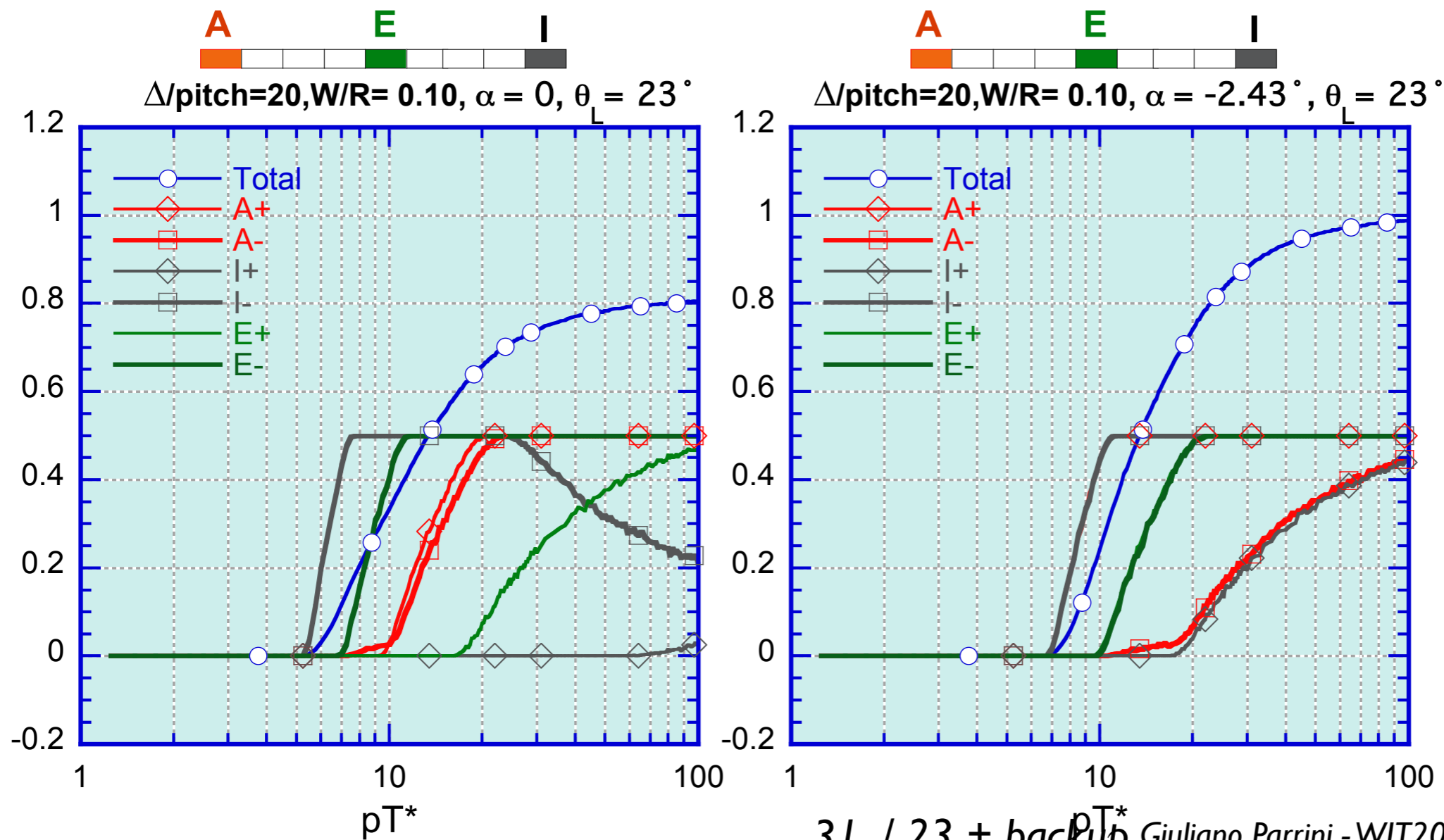


ToP = 40
N = 3

Selection efficiency and the Lorentz compensation

In the stacked detectors the Lorentz spread can be compensated either mapping or rotating the detector. The necessity of the compensation is important in case the signals are generated by electrons ($\theta_L \approx 23^\circ$).

The Lorentz spread impacts uniformly on all the detector. Particularly critical are the side areas where the acceptance perturbations are stronger.



ToP = 20

N = 3

$2D/\Delta = 0.1$

$\theta_L = 23^\circ$

$\alpha = -2.43^\circ$

Lorentz Compensation by tilting : single sensor

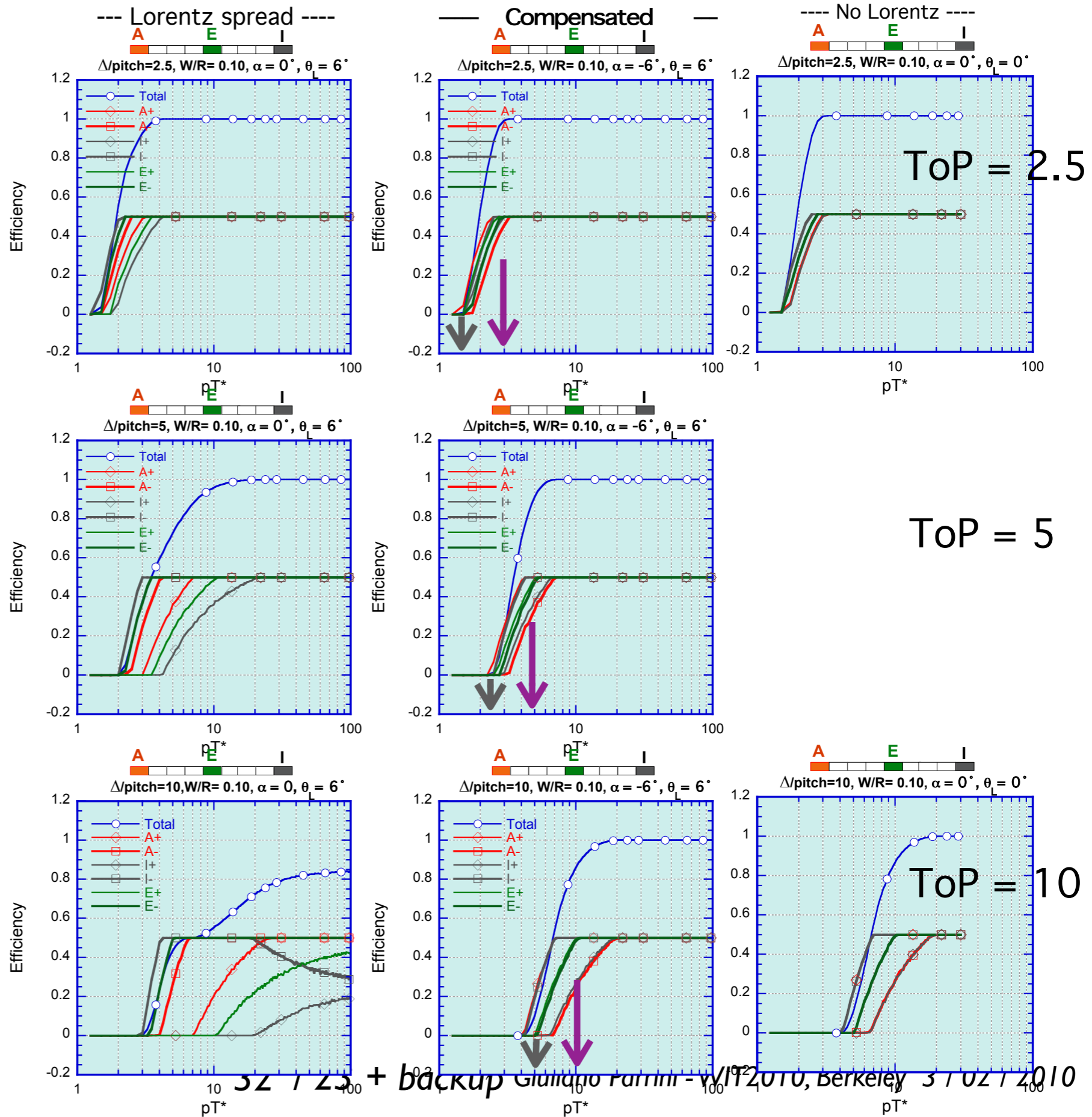
$$W/R = 0.1$$

$$N = 3$$

$$\theta_L = 6^\circ$$

$$\alpha = -6^\circ$$

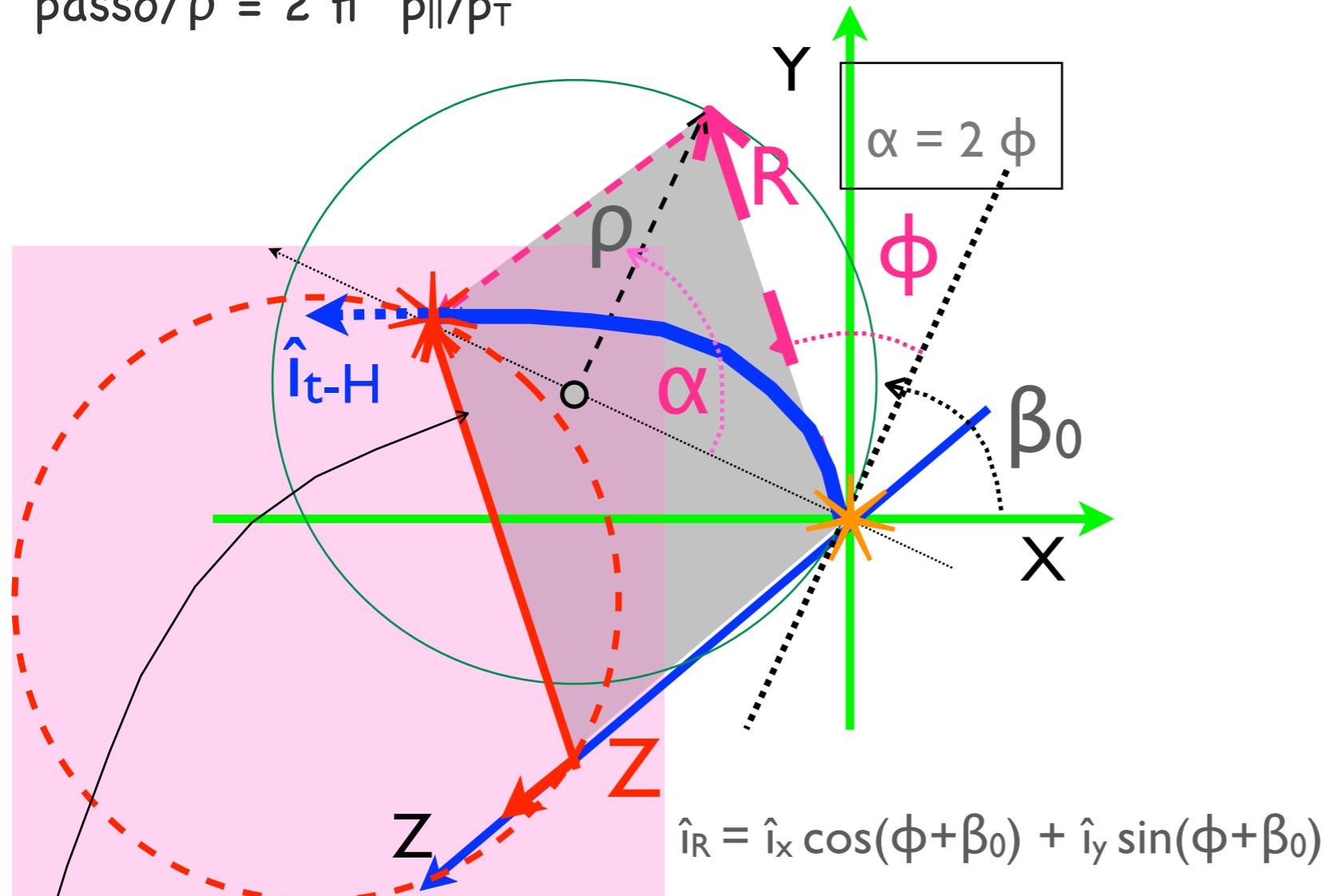
High thresholds high distortions and good compensation (but acceptance effects)



Cylindric helix trajectory

$$p_T(\text{GeV}/c) = 1.2 \rho(\text{m})$$

$$\text{passo}/\rho = 2\pi p_{||}/p_T$$



parametric equations

$$X = 2\rho \cos(\phi + \beta_0) \sin(\phi)$$

$$Y = 2\rho \sin(\phi + \beta_0) \sin(\phi)$$

$$Z = \text{passo} \frac{\phi}{\pi}$$

\hat{i}_{t-H} components

$$\frac{\partial X}{\partial s} = \frac{\cos(2\phi + \beta_0)}{\sqrt{1 + (p/2\pi\rho)^2}}$$

$$\frac{\partial Y}{\partial s} = \frac{\sin(2\phi + \beta_0)}{\sqrt{1 + (p/2\pi\rho)^2}}$$

$$\frac{\partial Z}{\partial s} = \frac{p/2\pi\rho}{\sqrt{1 + (p/2\pi\rho)^2}}$$

$$R = 2\rho \sin\phi$$

$$= (p_T/0.6) \sin(0.6 Z/p_{||})$$

$$\approx (p_T/p_{||}) Z$$

33

$$\frac{W_{R\Phi}}{R} = -\frac{\Delta Z}{Z} \sin^{-1}\left(\frac{p_T \min}{p_T}\right)$$

/ 23 + backup Giuliano Parrini - WIT2010, Berkeley 3 / 02 / 2010

sensor plane with γ gradient

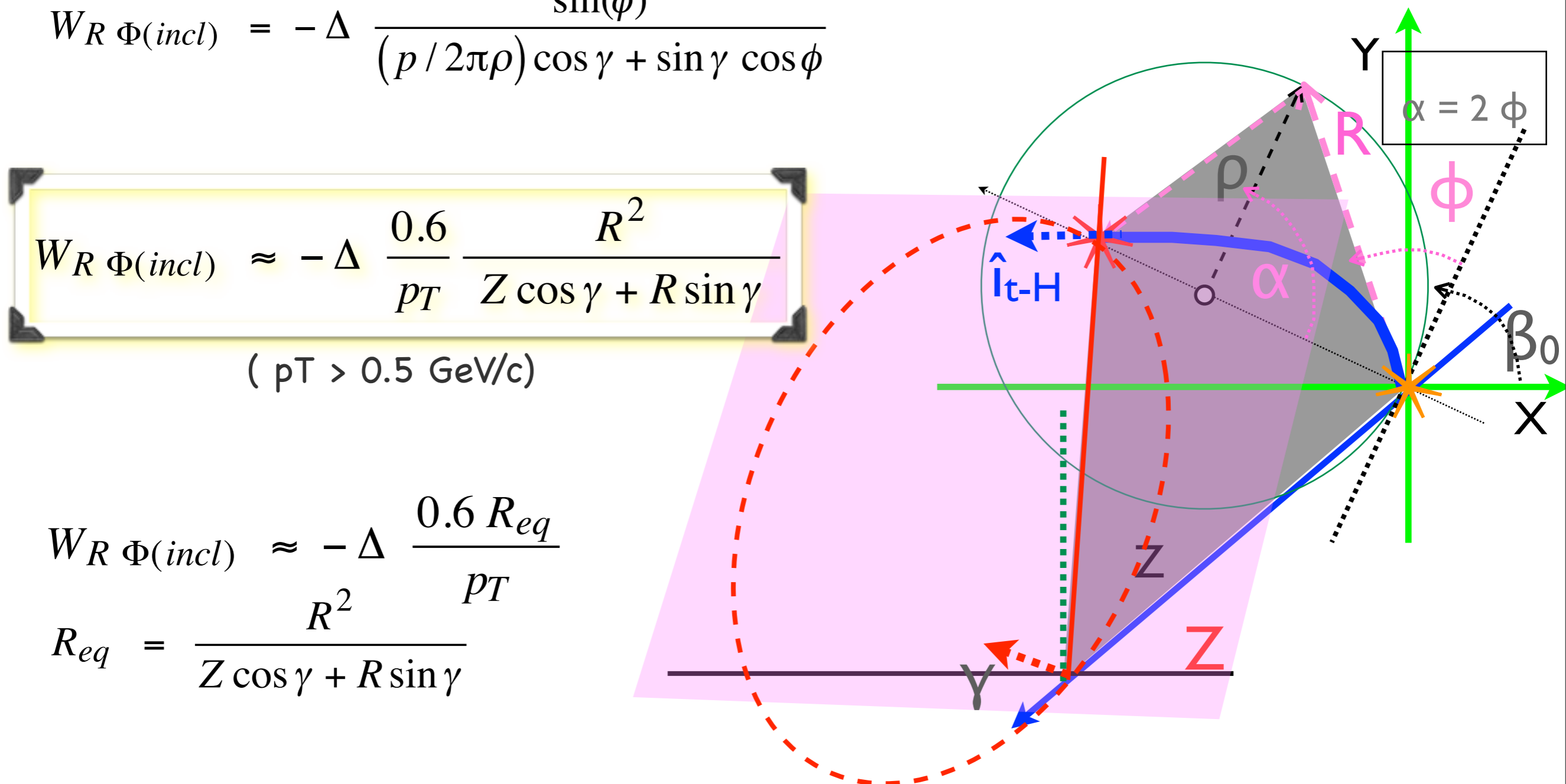
$$W_R \Phi(incl) = -\Delta \frac{\sin(\phi)}{(p/2\pi\rho) \cos \gamma + \sin \gamma \cos \phi}$$

$$W_R \Phi(incl) \approx -\Delta \frac{0.6}{p_T} \frac{R^2}{Z \cos \gamma + R \sin \gamma}$$

($p_T > 0.5 \text{ GeV}/c$)

$$W_R \Phi(incl) \approx -\Delta \frac{0.6 R_{eq}}{p_T}$$

$$R_{eq} = \frac{R^2}{Z \cos \gamma + R \sin \gamma}$$



R-Z map (10x10 cm²) : disc geometry

$$p_{Tth}/ToP \geq f(\text{GeV}/c) \approx 0.6 R^2/Z$$

f

○ ≥ 1.1

○ ≥ 1

○ ≥ 0.9

○ ≥ 0.8

○ ≥ 0.7

○ ≥ 0.6

○ ≥ 0.5

○ ≥ 0.4

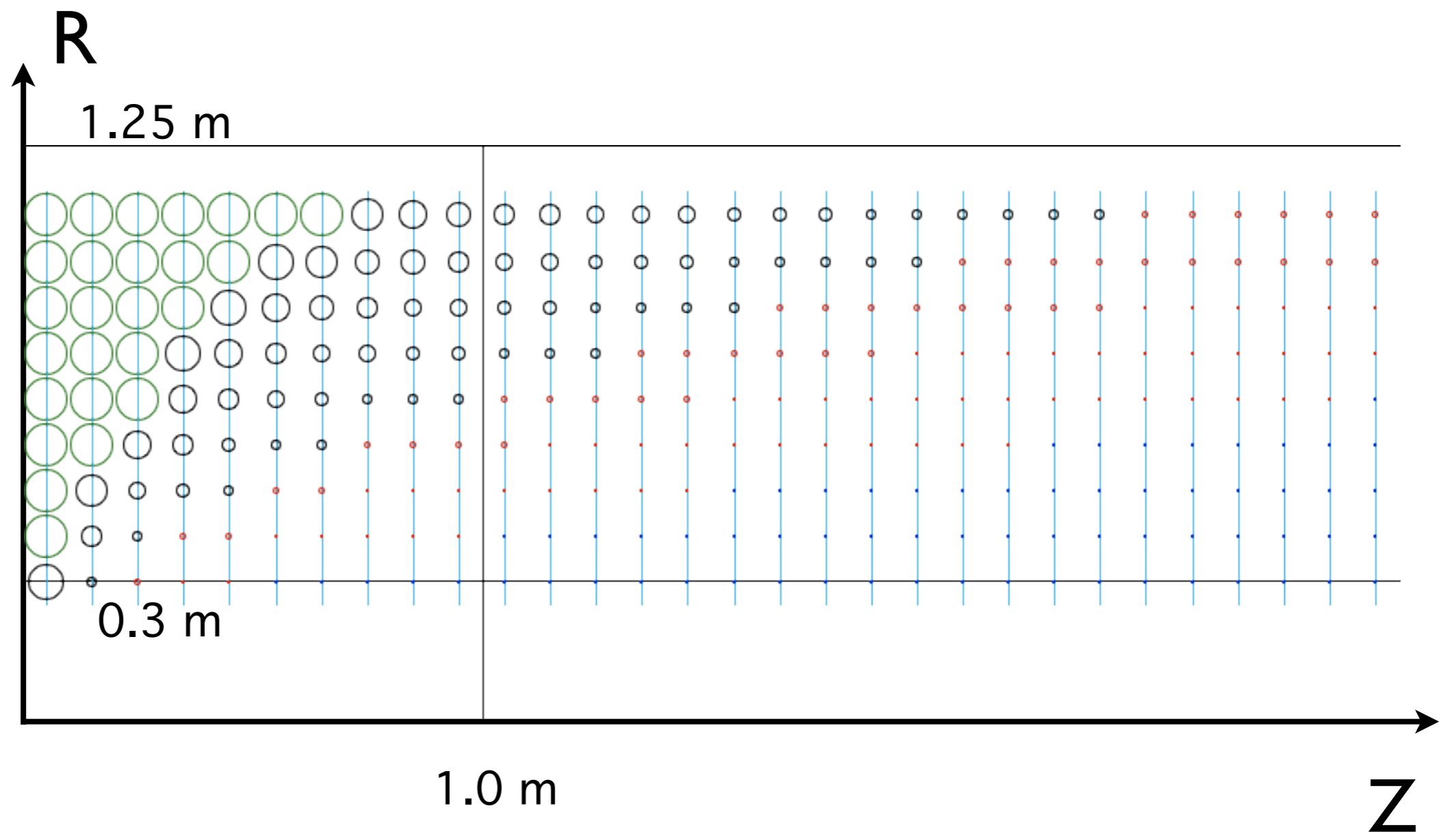
○ ≥ 0.3

○ ≥ 0.2

○ ≥ 0.1

○ < 0.1

$$p_{Tth100\%} = ToP \times f, \quad CW \leq 2 \text{ strip}$$



R-Z map (10x10 cm²) : disc/barrel like geometry

$$p_{Tth}/ToP \geq f(\text{GeV}/c) \approx 0.6 \times 1.1$$

$$p_{Tth100\%} = ToP \times f \quad , \quad CW \leq 2 \text{ strip}$$

